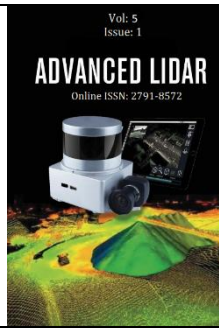
Advanced LiDAR
https://yakarm.com/journals/lidar
e-ISSN: 2791-8572
Volume 5, Number 1, pages 10-24



Research Article /Review Article:

Terrestrial Laser Scanning in Civil Engineering: Applications and Spatial Modeling

Shah Wali Nazari [*1] , **Veli Akarsu** [2]
[1] *Department of Geomatics Engineering, Institute of Science, Zonguldak Bülent Ecevit University, 67100 Zonguldak, Türkiye, e-mail: eng10501@gmail.com*
[2] *Department of Architecture and Urban Planning, Zonguldak Vocational School, Zonguldak Bülent Ecevit University, 67100 Zonguldak, Türkiye, e-mail: akarsu@beun.edu.tr*
* Correspondence: eng10501@gmail.com

Article History:
Received: 09.08.2025
Revised 1: 08.10.2025
Revised 2: 14.10.2025
Published: 23.10.2025

Keywords:
Terrestrial Laser Scanning;
Point Clouds;
Civil Engineering;
Structural Health Monitoring;
Deformation Monitoring.

This article is an open-access article distributed under the terms and conditions of the Creative Commons Attribution 4.0 International License (CC BY).

Publisher's Note:
This Journal remains neutral with regard to jurisdictional claims in published maps and institutional affiliations.

Abstract

Terrestrial laser scanning (TLS) has evolved over the past two decades from a specialised survey instrument into a core measurement technology for civil engineering practice. By capturing millions of three-dimensional (3D) points per second without physical contact with the object, TLS overcomes the discrete-point limitations of conventional total-station and GNSS surveying and enables rapid, low-cost acquisition of complete 3D geometric and visual information. This paper reviews terrestrial laser scanning technology, its measurement principles, scanner classification, system components and point-cloud data with a particular focus on its applications in civil engineering: structural health monitoring and deformation measurement, scan-to-BIM and digital-twin production, bridge and infrastructure inspection, construction-progress and earthwork-quantity tracking, and restoration and cultural-heritage documentation. Representative examples are drawn from the literature and from a complete field-to-model TLS case study carried out by the authors at Bülent Ecevit University- the exterior survey of the Farabi Mosque using a FARO Focus 3D X330 scanner - alongside a description of a current representative market instrument, the FARO FocusS 350. The review shows that TLS has matured into an accurate, versatile and cost-effective tool that is increasingly embedded in digital-twin and building-information-modelling (BIM) workflows across the civil engineering sector.

Copyright © 2025 by the author(s).

Contribution to the field statement:
This review examines terrestrial laser scanning (TLS) principles, technologies, and applications across civil engineering, supported by a field-to-model survey of the Farabi Mosque. By comparing point-cloud registration methods, it demonstrates how data cleaning and registration strategies influence practical accuracy, informing more reliable 3D documentation, deformation monitoring, and digital-twin workflows.

Highlights:

- TLS principles and applications across civil engineering are reviewed.
- Five point-cloud registration methods are compared in a mosque survey.
- Manual registration after data cleaning achieves a mean error of ±4.1 mm.
- Practical accuracy depends on workflow as well as scanner specifications.

Cite this article?
Nazari, S. W., & Akarsu, V. (2025). Terrestrial laser scanning in civil engineering: Applications and spatial modeling. Advanced LiDAR, 5(1), 10–24.

1. Introduction

Terrestrial laser scanning (TLS) is a new technology, developed since the early 2000s, for clear and precise distance and angle measurements in surveying and mapping applications. TLS uses laser pulses to measure distance and three-dimensional (3D) position (x, y, z), working at millimetre accuracy over distances of hundreds of metres.

The laser-scanner market for terrestrial applications has developed very successfully in recent years, and laser scanners are now regarded as measuring instruments that meet the requirements of industrial applications. A direct comparison of the various products is difficult because their technical specifications and physical measurement principles differ. Most systems consist of a combination of a distance-measurement system and a mechanical beam-deflection system that directs the laser beam in different directions and measures the distance to the nearest object for each direction.

Recent developments in terrestrial laser scanners are increasing their adaptation to many application fields. Unlike well-known geodetic instruments (e.g., total stations, GNSS receivers), the accuracy, resolution and performance of most existing laser scanners have not yet been fully demonstrated, and only a few systems have had their performance and manufacturer specifications confirmed by independent institutions. A comprehensive inspection and control procedure has not yet been developed; therefore, only individual tests report the results of existing systems.

In its present form, TLS has been developed by commercial instrument manufacturers such as Faro, RIEGL, Leica Geosystems, Zoller + Fröhlich and others. The capability of TLS has also been extended to the spectral domain through research leading to the development of multispectral and even hyperspectral lidar instruments [1]–[3].

Since the early 2020s, the scope of TLS has broadened considerably: it has become a cornerstone of digital-twin and building-information-modelling (BIM) workflows, of structural health monitoring of civil infrastructure, and of permanent (continuous) laser scanning, with growing adoption in autonomous mapping and GNSS-denied indoor scanning [4]–[6].

2. Methodology and System Architecture

This section describes the classification of terrestrial laser scanners, static and kinematic scanning, the components of a TLS system, point clouds and a representative instrument available on the market.

2.1. Classification of terrestrial laser scanners

A direct classification of terrestrial laser scanners is difficult. Several criteria are available: for example, the measurement principle (triangulation, phase-shift or time-of-flight) or other technical characteristics. There is no single instrument designed for all application fields. Some scanners are intended for indoor use at medium range (up to 100 m), some for outdoor use (up to 100 m), and some are high-precision close-range scanners (down to a few metres). Selecting the appropriate scanner for the application is essential. Terrestrial laser scanners can be categorised by their distance-measurement principle; the distance-measurement system is related to both the measurement range and the accuracy. Three different technologies are used for distance measurement:

- The most common laser measurement system is the time-of-flight (ToF) principle. This technique allows precise and clear distance measurements up to hundreds of metres and provides reasonable accuracy even for long-range scanning.
- In addition to the ToF principle, the phase-shift measurement principle represents the other common technique for medium-range measurements. Its measurement range is limited to about 100 m, and the accuracy of the measured distance is a few millimetres.
- Close-range laser scanners measuring up to a few metres also exist; these are used in industrial applications and reverse engineering (online monitoring of structural processes). Their distance-measurement principle is optical triangulation, a technique sensitive down to micrometres.

2.2. Distance-measurement principles and mathematical basis

The three ranging technologies introduced above can be expressed through their governing physical relationships. In the time-of-flight (ToF) principle, the distance d to the target is obtained from the round-trip travel time Δt of the emitted pulse and the speed of light c in the medium:

$$d = \frac{c\Delta t}{2}$$

In the phase-shift principle, the range is recovered from the phase difference Δφ of a continuously modulated wave, where f is the modulation frequency, λ the modulation wavelength and N the integer number of full wavelengths within the measured distance:

$$d = \frac{c}{2f}\frac{\Delta\varphi}{2\pi} = \frac{\lambda}{2}\left(N + \frac{\Delta\varphi}{2\pi}\right)$$

In close-range optical triangulation, the distance is derived from the fixed scanner base length b and the two angles α and β subtended at the emitter and the detector toward the object point:

$$d = \frac{bsin(\alpha)sin(\beta)}{sin(\alpha+\beta)}$$

Once individual scans have been acquired, point clouds captured from different stations are combined by a rigid-body transformation that maps each source point onto the common target frame using a 3×3 rotation matrix R and a 3×1 translation vector T:

$$P_{target} = RP_{source} + T$$

The quality of this registration is commonly quantified by the root-mean-square error (RMSE) of the residuals over the N matched points, which underlies the point-error figures reported later in the worked example (Table 1):

$$RMSE = \sqrt{\frac{1}{N}\sum_{i=1}^{N} \|P_i^{target} - (RP_i^{source} + T)\|^2}$$

The practical consequences of these three principles for civil-engineering work are summarised in Table 1, which contrasts their operational range, ranging precision, measurement rate and typical field applications.

Table 1. Comparison of the three terrestrial-laser-scanning distance-measurement principles and their typical civil-engineering applications.

Measurement principle	Operational range	Ranging precision	Measurement rate (points/s)	Typical civil-engineering use
Time-of-flight (ToF)	Long range (100 m – 2000 m+)	cm to sub-cm (±4–8 mm)	Moderate (10^4–10^5)	Mining, rockfall, landslide and dam monitoring
Phase-shift	Medium range (0.6 m – 150 m)	Millimetric (±1–2 mm)	Very high (~10^6)	Building documentation, scan-to-BIM, façade analysis
Optical triangulation	Close range (0.1 m – 5 m)	Sub-millimetric (≤0.1 mm)	High (~10^5)	Reverse engineering, precise structural-element inspection

2.3. Static and kinematic laser scanning

A further classification distinguishes static laser scanning, mobile laser scanning and kinematic laser scanning. In kinematic laser scanning the scanners are mounted on cars, helicopters, aircraft and boats; trajectory tracking is combined with total stations, GNSS and other sensors. Mobile mapping systems also incorporate Inertial Navigation Systems (INS) and optical-correlation-based positioning systems. Table 2 shows the application fields of terrestrial static and kinematic laser scanning.

Table 2. Terrestrial static and kinematic laser scanning and application fields

Scanning type	Range	Application fields
Kinematic – mobile mapping	various	Road/traffic monitoring, city modelling, mining monitoring
Kinematic – vehicle / platform	various	Infrastructure and route monitoring
Static	Long range (150–1000 m)	Facility management, industry, construction engineering, geology
Static	Medium range (50–150 m)	Building documentation, deformation control, heritage recording
Static	Short range (0–50 m)	Reverse engineering, body scanning, medicine, forensics

2.4. Components of a terrestrial laser scanner

A terrestrial laser scanner system (TLS) consists of the following components: scanning unit (scanner), power supply, tripod, and target spheres / target squares. The scanning unit is structurally larger than familiar measuring instruments and is the essential component of a TLS, being the system used to capture 3D data directly. A laser scanning unit comprises two components [7], [8]: the laser telemetry (laser distance-measurement system) and the laser beam-deflection unit (optical-mechanical scanner).

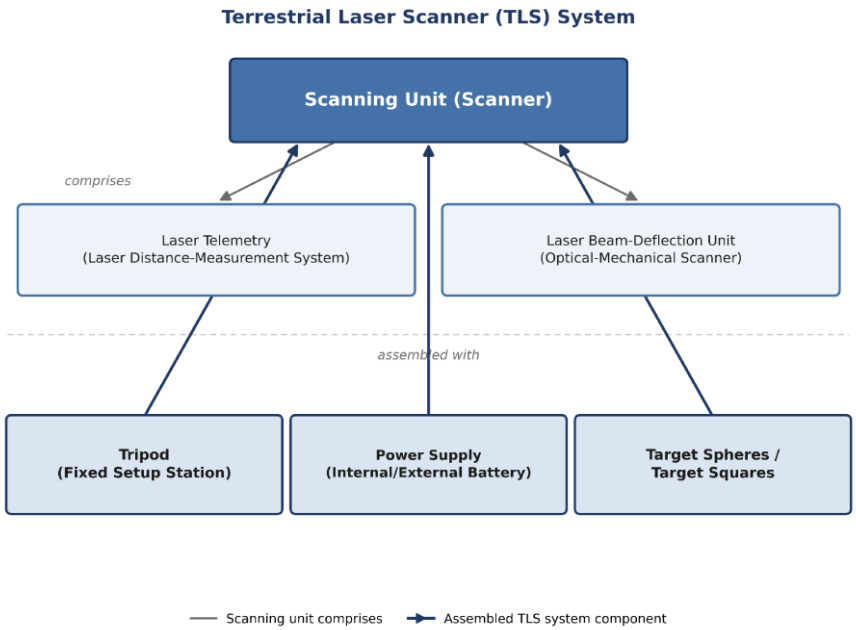


Figure 1. Main components of a terrestrial laser scanning (TLS) system: scanning unit, tripod, power supply, and target spheres/squares.

2.5. Point cloud

A laser scanner can be defined as a motorised total station. It obtains the surface data of the scanned object as 3D coordinates. The scanning process is automatic and systematic, converting thousands of (x, y, z) point coordinates per second. The high-density set of points obtained from terrestrial laser scans is usually collected as a point cloud during scanning and can be viewed simultaneously in the scanning software [6].

A point cloud is the sum of the (x, y, z) coordinates of an object or location within the general reference system of its spatial distribution. A point cloud contains various types of information [5]:

- Metric: describes the object geometry and shows the spatial relationships between objects in the environment.
- Visual or thematic: can be used to compute the reliability of the distance data for each point and to describe the properties of the object surface; additional information such as intensity or RGB (red, green, blue) values is also attached.

From the data of the generated point cloud, plans and elevation views can be produced for the desired or necessary parts.

2.6. Models on the market – FARO FocusS 350

The FARO FocusS 350 has been specially designed for outdoor applications owing to its small size, extra-light weight and extended scanning range. It enables scanning even in demanding environments — rainy or direct sunlight conditions, narrow work sites, dusty or humid areas. An on-site compensation tool allows on-site data-quality optimisation. Integrated GNSS and GLONASS receivers enable easy positioning, while HDR imaging and HD photo resolution provide real-detail scanning results with high data quality. Distance accuracy up to ±1 mm; range from 0.6 m to 350 m; HD photo overlay up to 165 megapixels; 2017 model. The FocusS 350 is presented here as a representative current TLS instrument, illustrating the capability of modern systems on the market; the field survey reported below in the Worked Example section was carried out with an earlier-generation FARO instrument available to the authors at the time, the Focus 3D X330 (2013 model), whose specifications are given in that section.

3. Application Fields

TLS is increasingly used for 3D modelling of indoor and outdoor environments, building documentation, volumetric and dimensional control of excavations, documentation of deformation processes, building facade inspection, inspection of load-bearing capacity and wear of supporting structures, monitoring of the construction process for legal and technical documentation, virtual exhibition of historical sites for restoration and scientific analysis, accident and crime-scene investigation, and in ever new fields. In detail:

- Control of the conformity of projects to the site, comparison of construction progress with plans and quality control.

• Spatial analysis of the situation involving virtual planning and existing terrain relations (combined structures, multi-storey transport centres, shopping centres, etc.).
• Establishment of building information systems aimed at interactive structural investigation, risk detection and decay control for the proper maintenance of buildings and structures [4].
• Documentation of industrial environments to create a visual 3D factory — a complete digital model of an existing factory or plant, enabling new equipment to be programmed and work to continue without stopping production, and updating outdated drawings to match reality.
• Documentation of a country's infrastructure facilities (railways, road networks, tunnels, bridges, power lines), providing a basis for assessment methods that identify damaged areas so that necessary repairs can be completed without delay.
• Deformation control of the object or area to be scanned, which can often be analysed with terrestrial laser scanners without discrete points, so that local deformations can be revealed.
• Detailed condition and damage assessment of historical heritage (churches, castles, palaces, etc.), preparation of the documentation necessary for their preservation, and provision of restoration at any given time in the future in case of damage or destruction; accurate, realistic, visual 3D models also enable virtual tourism of historical heritage via the internet [8].
• Part control: produced parts generally have very different shapes and sizes, so part control for accuracy and quality assurance is carried out with flexible 3D metrology tools.

3.1. Use in rockfall studies

This study was carried out in the Vall de Núria valley in Spain, where rockfall frequently occurs, on a 300×500 m area, using a long-range Optech Ilris3D TLS to evaluate the rockfall phenomenon and to apply preventive and corrective measures [9], [10].

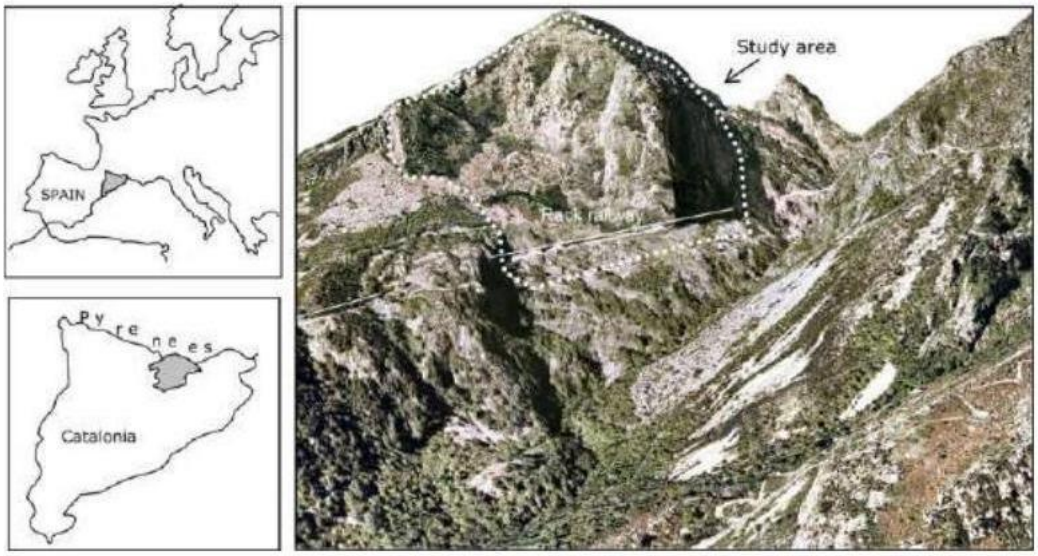


Figure 2. Study area at Vall de Núria, Eastern Pyrenees, Spain. The pilot area is surrounded by a dotted line.

3.2. Use in building structure documentation

TLS techniques have proven effective in building structure documentation, building deformation studies, natural-disaster studies and cultural heritage studies [5]. Building documentation yields valuable information for various civil-engineering topics (urban planning, restructuring, monitoring, conservation and restoration of cultural-heritage buildings). Reliable and detailed 3D models are produced to obtain detailed data (material types, comprehensive determination of the structure), and the data obtained can be integrated into CAD systems for measurement or change and alteration studies (e.g., 3D models of cultural structures acquired before and after restoration).

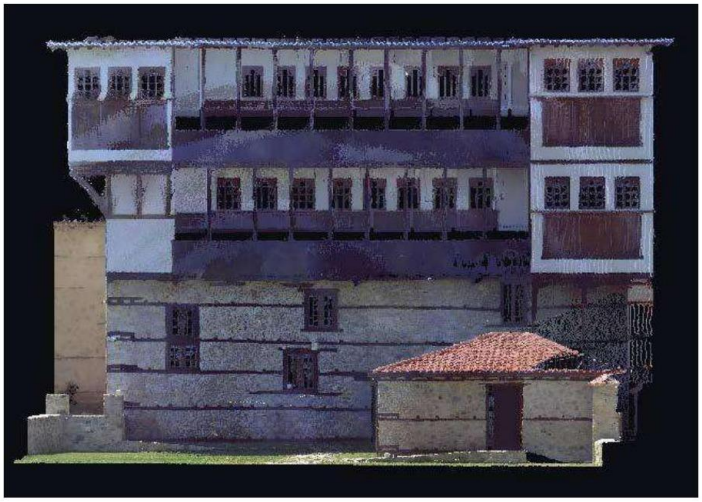


Figure 3. Tsiatsiapa historical building – front-facade 3D data cloud.

3.3. Use in cultural heritage preservation

Laser scanners are increasingly used as a versatile tool in the preservation of cultural heritage. In particular, old buildings and archaeological sites are scanned for data archiving, precise modelling and simple visualisation, and recent practice-based guides now explicitly bridge TLS data capture with HBIM, VR and AR integration [11].

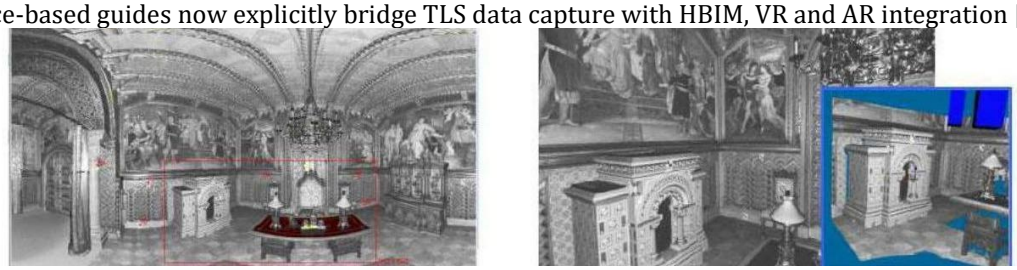


Figure 4. Three modes of the scanned image: left, "overview mode"; right, "perspective mode"; thumbnail, 3D point cloud.

3.4. Use in traffic control

Laser scanners are increasingly used as measuring instruments for various applications in traffic-regulation analysis. In particular, tunnels and road conditions are subject to continuous monitoring. As traffic increases, the infrastructure must be kept in proper condition and the traffic network (bridges, tunnels, etc.) must be monitored in detail.

3.5. Use in measuring forest structure

Besides airborne laser scanning, terrestrial laser scanning is also used in forestry. Terrestrial laser scanners are used for fast, efficient and basic inventory determination, and for measuring parameters such as tree count and position, diameter at breast height (DBH), tree height, and trunk and canopy height, with recent work benchmarking competing TLS-derived vegetation-index methods against hemispherical photography across hundreds of trees [12].

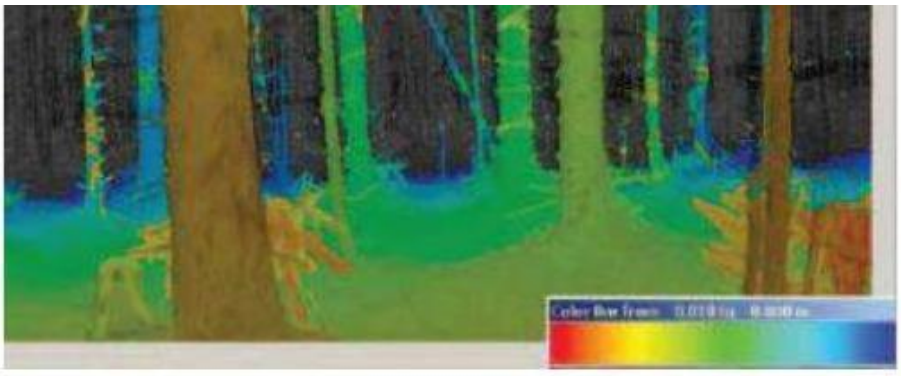


Figure 5. Range image of a tree-species mixture; maximum range 8 m (red, 1 m from scanner; blue, 8 m from scanner).

3.6. Use in landslide detection and monitoring

In landslide monitoring, GNSS techniques produce highly accurate results. However, large mass landslide movements destroy or lose polygon points, in which case the monitoring process cannot continue. TLS techniques are more suitable in such situations because they do not depend on polygon points in the landslide area. Their greatest advantage is the fast and precise scanning of the entire large landslide area; multiobjective optimisation of TLS scan-station placement has further improved coverage over complex landslide terrain [13].

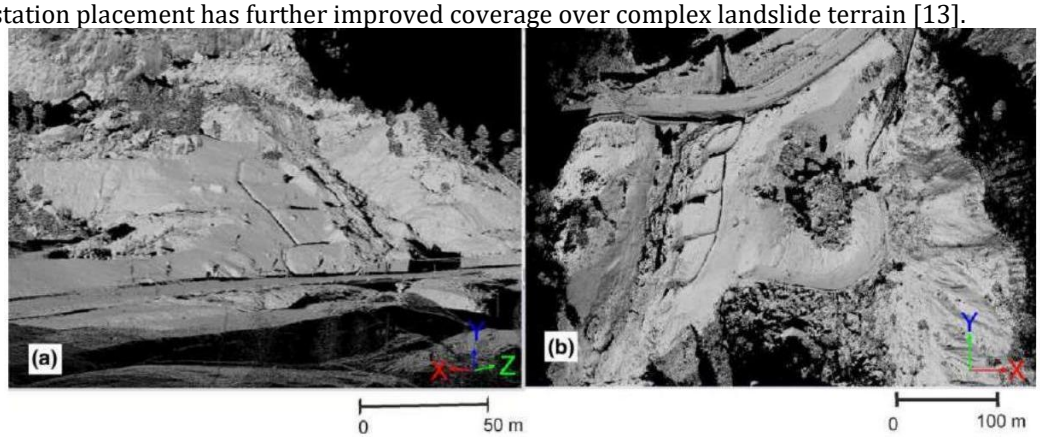


Figure 6. Point cloud of the 2011 landslide at Taşkent, Konya: (a) perspective view, (b) top view.

3.7. Use in tunnels

TLS is used in construction and repair-maintenance management in tunnels. In the near future, laser scanning will probably be used as a standard tool for geological and geodetic analyses in tunnels. TLS applications in tunnels include determining the geological characteristics of tunnels, monitoring the geometry of tunnels during excavation, and making deformation measurements; automated filtering of TLS point clouds now supports real-time over-break/under-break detection during drill-and-blast excavation [14].

3.8. Use in monitoring coastline changes

Changes in coastal profiles under the influence of regular and irregular waves have been studied by many researchers, both experimentally and with the help of numerical modelling, for many years. Field and laboratory studies show that measurement methods are insufficient to determine the net solid-transport amount precisely. In the study, the change of the coastal profile under the influence of an irregular wave of known height and period was measured with a terrestrial laser scanner.

3.9. Use in mining

TLS can be used to calculate volumetric and surface-change comparisons of earthworks in mines. In a gold-mining operation in East Africa (Tanzania), it was used for scanning positioning, filtering and analysis. Area and volume calculations and the analysis of the results for a six-month period are presented, and Multi-Criteria Surface Analysis (MSA) to evaluate the accuracy of the scans is discussed; more recently, combining TLS with UAV photogrammetric point clouds has improved volumetric material reconciliation at open-cut mines [15].

3.10. Emerging application areas (2021–2025)

Beyond the classical fields above, TLS has expanded into new domains in recent years. The technology now underpins geometric digital-twin generation for reinforced-concrete infrastructure [4] and LiDAR-based structural health monitoring of bridges, tunnels and post-disaster reconnaissance [5]. Permanent (continuous) laser scanning and 4D point-cloud analytics have enabled automated detection of recurring surface dynamics, while long-term high-Alpine rock-wall monitoring has quantified erosion and rockfall linked to permafrost degradation over nearly two decades [16]. On the indoor and autonomous side, TLS is increasingly used as a ground-truth reference for benchmarking LiDAR-SLAM algorithms in GNSS-denied environments [6], and multispectral TLS coupled with radiative-transfer modelling now maps 3D canopy biochemistry throughout the canopy volume [3].

4. Civil Engineering Applications

Civil engineering is one of the disciplines where TLS has moved furthest beyond simple documentation, becoming embedded in monitoring, design and asset-management workflows that run from a single point cloud through to a maintained digital twin. This section brings together, and expands on, the civil-engineering-relevant material introduced above under five focus areas: structural health monitoring and deformation measurement, scan-to-

BIM/HBIM and digital-twin production, bridge and infrastructure inspection, construction-progress and earthwork-quantity tracking, and restoration and cultural-heritage documentation.



Figure 7. Terrestrial-laser-scanning workflow from point cloud acquisition to digital twin, underlying the scan-to-BIM and digital-twin applications discussed below.

4.1. Structural health monitoring and deformation measurement

TLS is increasingly embedded in structural health monitoring (SHM) programmes for buildings, dams and bridges. Because a scanner records dense, geo-referenced point clouds of an entire surface rather than a set of discrete targets, repeat epochs of the same structure can be co-registered and differenced to produce full-field displacement and deformation maps, revealing localised movements — settlement, tilt, crack opening or bulging — that would be missed by conventional point-wise instrumentation such as extensometers or total stations [5]. Complementary laboratory work on retaining walls has shown that, with a carefully chosen scanning distance and incidence angle, TLS can resolve geometric surface anomalies to within 1–2 mm, supporting its use for serviceability-limit-state monitoring of earth-retaining structures [17]. Multi-epoch and permanent (continuous) TLS installations extend this capability to long-term monitoring, tracking millimetre-scale deformation trends over months or years and supporting early-warning thresholds for critical infrastructure [16].

4.2. Scan-to-BIM, HBIM and digital-twin production

Registered TLS point clouds provide the geometric backbone for scan-to-BIM workflows, in which as-built surfaces are segmented, fitted to parametric elements (walls, slabs, beams, piping) and assembled into building-information models that match real, rather than as-designed, geometry. For reinforced-concrete infrastructure such as box-girder bridges, this process can be automated to generate geometric digital twins directly from the scan data, linking the 3D model to inspection and maintenance records [4]. A 2025 field study on a newly built road bridge integrated TLS-derived point clouds into a Bridge Information Model (BrIM) linked to a decision-support dashboard, reporting a 37% increase in the accuracy of structural-anomaly detection, a 42% reduction in inspection and diagnosis time, and a 25% reduction in operational maintenance costs relative to conventional visual inspection [18]. Because scan quality and coverage strongly affect the reliability of the resulting model, recent work has also proposed BIM-driven scan-path planning, in which the design model itself is used to compute optimal scanner locations and station parameters before the survey begins, improving data completeness on large civil infrastructure such as suspension bridges [19]. For historic structures the same workflow underlies Historic/Heritage BIM (HBIM), which couples point-cloud-derived geometry with archival and material information and is now explicitly integrated with VR/AR visualisation in current heritage-documentation practice [11].

4.3. Bridge and infrastructure inspection

On bridges, tunnels and other transport infrastructure, TLS supplies dense as-built geometry for deck alignment, expansion-joint condition, clearance envelopes and deflection under load, complementing visual inspection with quantitative, repeatable measurements. In tunnels, TLS is used to determine geological characteristics, monitor the excavation profile against the design cross-section and detect over-break/under-break; recent work has automated the filtering of TLS point clouds to support near-real-time deformation detection during drill-and-blast excavation, directly supporting construction-safety decisions [14]. Mobile laser scanning has extended this capability to operational shield tunnels, where segmenting the point cloud by ring and tracking centreline shift and ovality between successive epochs enables continuous, ICP-based displacement analysis of the tunnel lining without interrupting service [20].

4.4. Construction-progress and earthwork-quantity tracking

On active construction sites, periodic TLS surveys are compared against the design or 4D-BIM schedule to verify that built geometry conforms to the plans, to quantify construction progress and to flag deviations for quality control. A 2025 case study on a residential building under structural erection combined drone-based laser scanning with 4D-BIM in an automated visual-programming pipeline, delivering a web-based digital-twin platform that gives site teams near-real-time access to progress deviations [21]. The same principle underlies volumetric monitoring of earthworks and excavations: point clouds from successive epochs are differenced to compute cut/fill and stockpile volumes, and combining terrestrial scans with UAV photogrammetric point clouds has been shown to improve the accuracy of volumetric material reconciliation on large open sites such as mines [15].

4.5. Restoration and cultural-heritage documentation

Within civil and restoration engineering, TLS underpins the structural condition assessment of historic buildings prior to retrofit or strengthening works, providing accurate baseline geometry for both structural analysis and conservation planning. Point clouds acquired before, during and after restoration allow engineers to verify that intervention works have achieved their intended geometric outcome and to maintain a permanent digital record of the structure for future reference, while HBIM-based documentation increasingly links this geometric record to material condition and maintenance history [11].

5. Case Study: Exterior TLS Survey of the Farabi Mosque, Zonguldak Bülent Ecevit University

To ground the review above in an original field deployment, this section presents a complete, field-to-model TLS case study carried out by the authors at Zonguldak Bülent Ecevit University (ZBEÜ): the exterior survey of the Farabi Mosque on the university's Farabi Campus [22]. The mosque is a three-storey structure with a genuinely difficult scanning environment, an open car park to the north, a vehicle road to the west, a pedestrian path to the east, and, on the south elevation, a clearance of less than one metre, a constraint that later limited the completeness of the resulting model on that side.

5.1. Site and instrument

The survey used a FARO Focus 3D X330 (2013 model) phase-shift terrestrial laser scanner, an earlier generation than the FocusS 350 introduced as a current market example in the Method section, but built on the same phase-shift measurement principle, borrowed from the Geomatics Engineering measurement laboratory with the department's permission. The instrument measures at up to 976,000 points per second over a range of 0.6–330 m, with a nominal ranging error of ±2 mm, and integrates a GPS receiver, compass and dual-axis compensator in a 5.2 kg unit controlled via touchscreen and WLAN (Figure 8).



Figure 8. The FARO Focus 3D X330 terrestrial laser scanner and accessories used for the Farabi Mosque survey. Adapted from [22].

5.2. Field workflow

Station positions were first planned remotely from Google Earth imagery and then verified during a site reconnaissance visit on 2 November 2019; scanning itself took place on 13 November 2019. Reference targets were white measuring spheres, positioned so that at least three spheres were common to every pair of overlapping scans, the condition that makes target-based registration possible afterwards.

Eight scan stations (SS005, SS006, SS007, SS009, SS010, SS011, SS012 and SS013) were occupied around the building, each scanned for ten minutes with the following parameters active on the instrument: outdoor profile, equal-weighted daily measurement mode, 29.1 Mpts/s, 4× quality, a full 360° (horizontal) × 180° (vertical) field of view, and full-colour capture, with the onboard GPS running throughout to geo-tag every station. Figure 9 plots the eight stations in the local coordinate frame recovered from the survey, together with an illustrative footprint of the mosque sized to the façade dimensions measured later in this section.

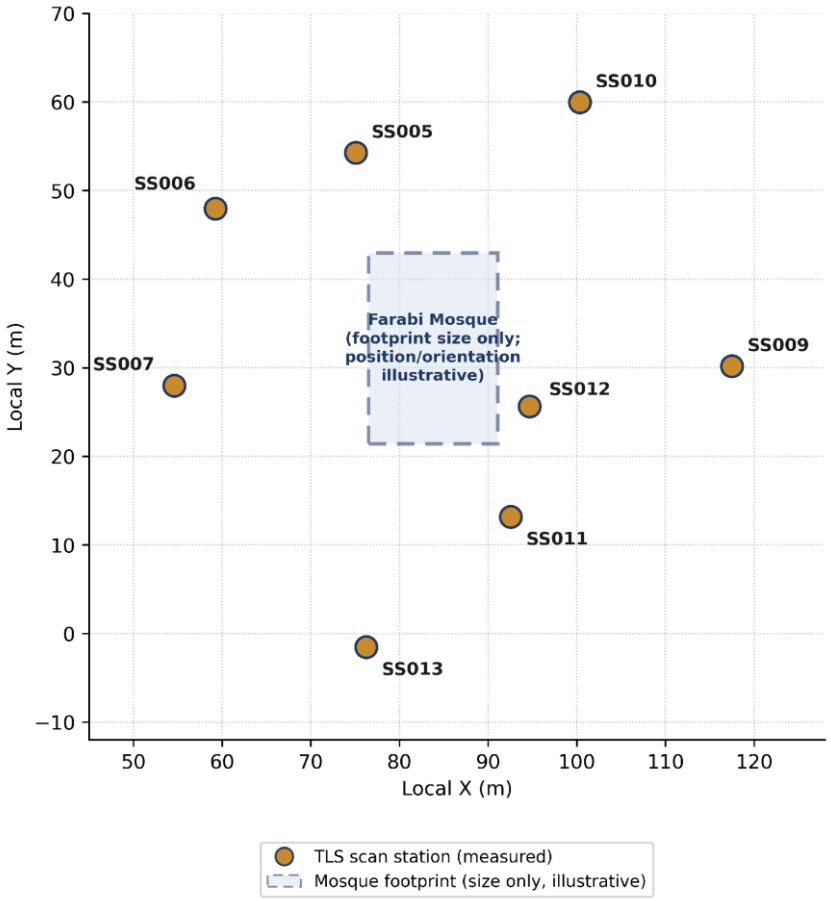


Figure 9. As-surveyed TLS scan-station layout for the Farabi Mosque, in the local coordinate frame recovered from the eight onboard-GPS station fixes; the shaded rectangle shows only the measured façade dimensions, not the mosque's true position or orientation, which were not part of the recovered dataset. Data from [22].

5.3. Registration and point-cloud processing

Back in the office, FARO Scene 2019 was used to merge the eight sessions. A first attempt at fully automatic registration on the raw, unedited scans failed to produce an acceptable model, because each scan also captured extraneous surrounding objects, parked cars, passers-by, vegetation — with no counterpart in the neighbouring stations. Polyline-selection and clipping-box tools in Scene 2019 were therefore used to strip these unwanted points from all eight sessions; the cleaned dataset retained 35,700,815 points.

On the cleaned data, four automatic registration strategies (Cloud-to-Cloud, Target-Based, Top-View, and Top-View-plus-Cloud-to-Cloud) were tested and compared with a manual, target-based registration in which common spheres and shared planar surfaces were matched by hand. Table 3 and Figure 9 summarise the results: manual target-based registration gave both the lowest point error (mean ±4.1 mm, maximum ±8.4 mm) and the best scan overlap (16.5%) of any method tried, while fully automatic registration attempted on the uncleaned scans was markedly worse (mean point error around ±12.3 mm, maximum ±15.7 mm, 23.0% overlap on the individual station pairs), a direct, field-measured illustration of the point made in the Discussion below, that TLS accuracy in practice depends heavily on pre-processing and registration strategy, not on instrument specification alone. Figure 10 shows the resulting registered point cloud.

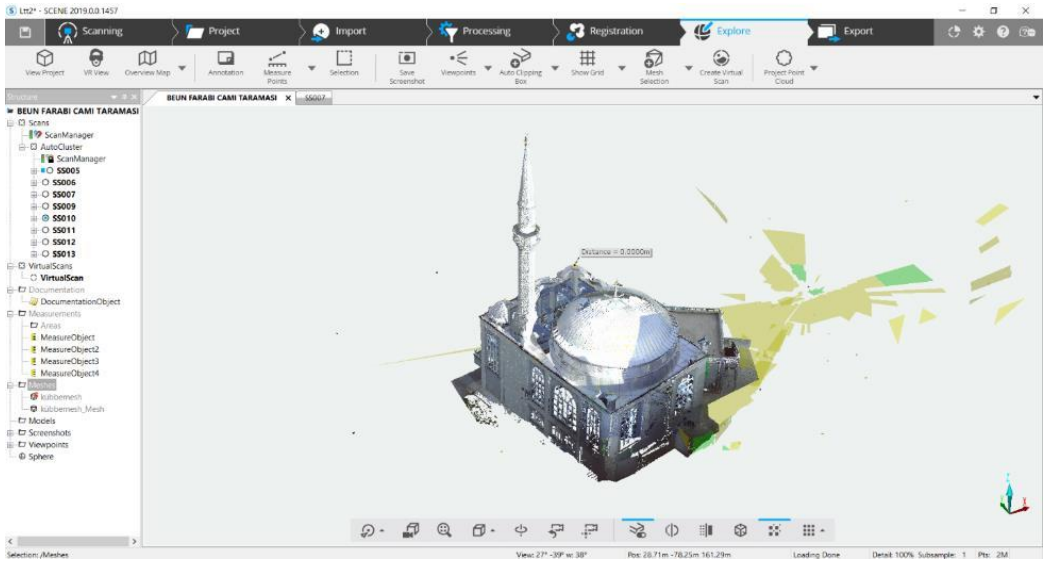


Figure 10. The Farabi Mosque exterior point cloud after point-cloud cleanup and manual, target-based registration of all eight scan stations. Adapted from [22].

Table 3. Comparison of point-cloud registration strategies tested for the Farabi Mosque survey (Faro Scene 2019)

Registration method	Max. point error (± mm)	Mean point error (± mm)	Min. overlap (%)
Cloud to Cloud	13.8	5.2	3.5
Target Based	16.8	6.9	5.9
Top View	32.9	13.3	10.9
Top View + Cloud to Cloud	11.6	5.5	10.8
Manual (Target Based)	8.4	4.1	16.5

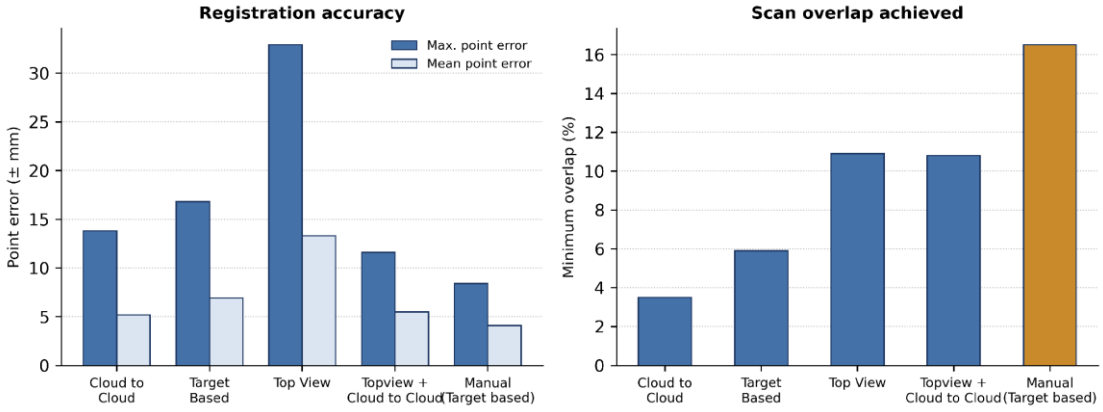


Figure 11. Point-cloud registration accuracy and overlap achieved by the five strategies compared in Table 3. Data from [22].

5.4. Deliverables and geometric measurements

The registered point cloud was exported in DXF and PTS formats for further work in Autodesk ReCap, Autodesk AutoCAD and Reconstructor: ReCap and AutoCAD were used for plan and section extraction and for length/area measurement, while volume calculation required Reconstructor's dedicated tools (Figure 12). Table 4 lists the principal geometric quantities measured directly on the 3D model.

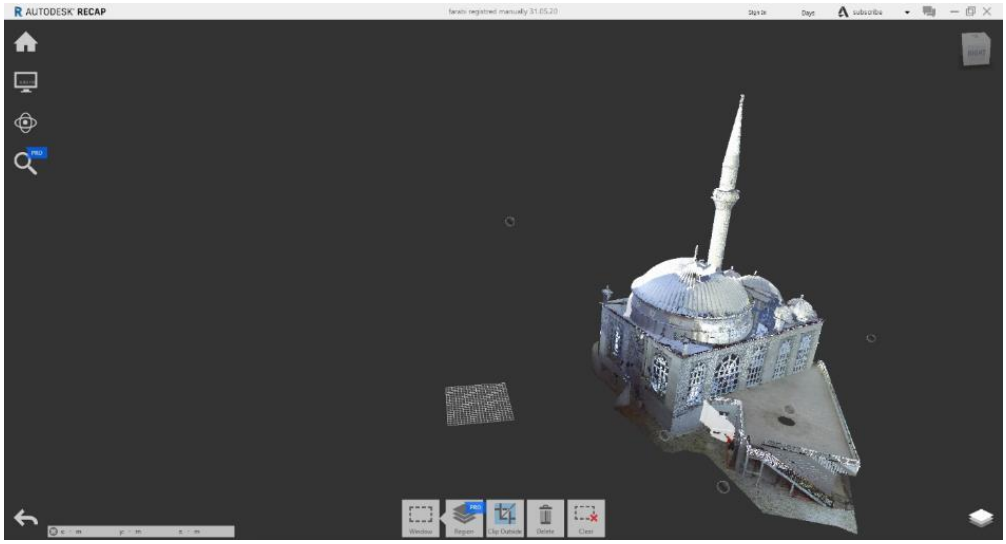


Figure 12. The registered Farabi Mosque point cloud imported into Autodesk ReCap for plan, section and metric measurement work. Adapted from [22].

The minaret height was measured twice, on two different software platforms working from the same registered point cloud: 24.940 m from a point-to-point Distance measurement in FARO Scene 2019 the same session used for the other geometric quantities in Table 4 and 22.050 m from an independent measurement in Autodesk ReCap, in which the minaret was first isolated with a crop-outside operation before applying the Distance tool. The 2.89 m (11.5%) gap between the two is far larger than the sub-centimetre point errors reported for registration in Table 3, so it cannot be explained by registration quality. Two factors are the most likely contributors. First, the crop-outside isolation applied in Autodesk ReCap may have unintentionally clipped the uppermost part of the minaret — its conical cap (külah) and finial (alem) — before the Distance tool was applied, which would systematically shorten the ReCap value; the crop boundary was not independently verified against the raw point cloud, so this cannot be excluded. Second, operator point-picking uncertainty at the minaret's narrow, tapering apex is amplified by the reduced point density on the mosque's south side, where the sub-one-metre survey clearance (see Lessons learned, below) caused occlusions and left that part of the model less complete. A limitation of this worked example is that no independent ground-truth value — for example, a trigonometric height obtained with a total station — was recorded on site, so it is not possible to determine which of the two software measurements is closer to the true minaret height; the figures should therefore be read as an internal cross-software comparison rather than as a validated height. More broadly, the discrepancy is a useful reminder that the point-cloud accuracy summarised in Table 3 describes the internal consistency of the registered dataset, not the accuracy of any single manually picked feature measurement extracted from it — a distinction that matters wherever TLS deliverables feed engineering decisions.

Each of the eight stations' onboard GPS also logged WGS-84 ellipsoidal coordinates, which were transformed into the shared local Cartesian frame used for registration and plotted in Figure 9; the associated coordinate standard deviations were generally at the few-millimetre to centimetre level, consistent with the registration accuracy reported above.

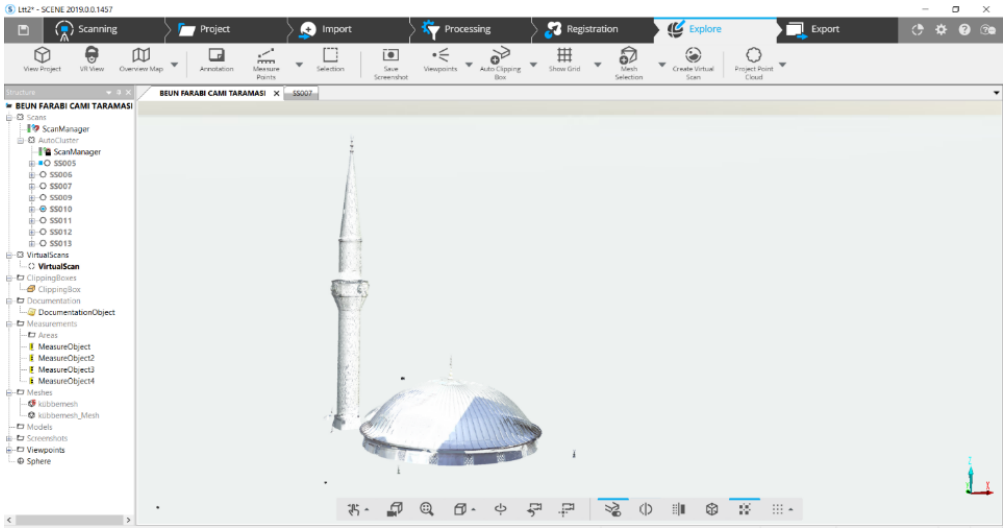


Figure 13. Cross-section through the dome and minaret extracted from the registered 3D model, used to derive the dome-diameter and minaret-height measurements in Table 4. Adapted from [22].

Table 4. Principal geometric quantities measured on the registered 3D model of the Farabi Mosque. Data from [22]

Measured quantity	Value
Front-façade length	14.580 m
Front-façade height	10.450 m
Side (west) façade length	21.554 m
Minaret height (FARO Scene 2019 measurement)	24.940 m
Minaret height (Autodesk ReCap measurement, isolated via crop-outside)	22.050 m
Large-dome diameter	13.650 m
Spacing between the two small domes	10.592 m
Front-façade area	148.820 m^2
Terrace area	139.310 m^2

5.5. Practical Considerations and Field Limitations

The authors draw three practical conclusions from this survey that generalise beyond the Farabi Mosque itself [22]. First, a site with less-than-one-metre clearance on one elevation common on urban and campus buildings will produce an incomplete model on that side regardless of scanner quality, and should be flagged during planning rather than discovered afterwards. Second, manual point-cloud cleanup before registration, while time-consuming, made the difference between a failed automatic registration and a usable model with millimetre-level accuracy; scan planning that avoids capturing unrelated objects in the first place (parked vehicles, passers-by) considerably reduces this later burden. Third, target markers should be placed so that they remain visible and connectable from every station that needs them, since registration quality depends directly on how many shared references each pair of scans has in common.

6. Discussion

The findings summarised above show that TLS has matured into a versatile, accurate and cost-effective measurement technology applicable across a wide spectrum of engineering, environmental and cultural-heritage disciplines. Its principal strength acquiring millions of accurate 3D points rapidly and without contact with the object addresses the limitations of conventional geodetic methods, total stations and GNSS, which provide only discrete point measurements and are therefore slower and less suitable for complex geometries [5], [7]. The case studies reviewed confirm that TLS delivers reliable geometric and thematic information for documentation, deformation monitoring and volumetric analysis, while remaining independent of control points in unstable areas such as landslides [13]. Nevertheless, a comprehensive, standardised procedure for evaluating the accuracy, resolution and performance of terrestrial laser scanners has not yet been established, and only a limited number of systems have been independently certified. The Farabi Mosque worked example presented above illustrates why this matters in practice: on the same instrument and the same dataset, point accuracy ranged from ±4.1 mm (mean, manual target-based registration after cleanup) to ±12.3 mm (mean, automatic registration on uncleaned scans) — an almost threefold difference driven entirely by pre-processing and registration choices rather than by the scanner itself [22]. This remains an open issue and a direction for future work, together with the integration of TLS with hyperspectral sensing [1]–[3], mobile mapping and building information modelling.

7. Conclusion

This study reviewed terrestrial laser scanning (TLS) technology, the design of terrestrial laser scanning systems, point clouds and their application fields, and presented examples from the literature and from work carried out at Bülent Ecevit University, including a complete field-to-model worked example — the exterior TLS survey of the Farabi Mosque in which manual, target-based registration after point-cloud cleanup achieved a mean point accuracy of ±4.1 mm against ±12.3 mm for automatic registration on uncleaned data, underscoring how strongly practical accuracy depends on workflow rather than on the scanner alone [22]. TLS, which emerged as a research field in the late 1990s and early 2000s, has become a popular and effective method for the documentation and 3D modelling of historical and cultural structures and for numerous engineering, environmental and forensic applications. Using terrestrial laser scanners, thousands of 3D points can be recorded in a very short time, enabling fast, accurate and low-cost acquisition of 3D geometric and visual information. With continuing advances in instrumentation and the development of multispectral and hyperspectral lidar, the range of TLS applications is expected to expand further.

Acknowledgements
The authors thank the Department of Geomatics Engineering, Institute of Science for their support and for providing access to the terrestrial laser scanning laboratory equipment used in this study.

Funding
This research received no external funding. The work was supported by the institutional resources of Zonguldak Bülent Ecevit University.

Conflicts of interest
The authors declare no conflict of interest.

Data availability statement
The data and point clouds presented in this study are available on request from the corresponding author. The data are not publicly available due to ongoing institutional research.

Institutional review board statement
Not applicable. This study did not involve humans or animals.

CRediT author statement
Shah Wali Nazari: Conceptualization, Methodology, Investigation, Writing – original draft. Veli Akarsu: Conceptualization, Supervision, Writing – review & editing.

References
[1] F. M. Danson, R. Gaulton, R. P. Armitage, M. Disney, O. Gunawan, P. Lewis, G. Pearson, and A. F. Ramirez, "Developing a dual-wavelength full-waveform terrestrial laser scanner to characterize forest canopy structure," Agric. For. Meteorol., vol. 198–199, pp. 7–14, Dec. 2014, doi: https://doi.org/10.1016/j.agrformet.2014.07.007.
[2] T. Hakala, J. Suomalainen, S. Kaasalainen, and Y. Chen, "Full waveform hyperspectral LiDAR for terrestrial laser scanning," Opt. Express, vol. 20, no. 7, pp. 7118–7127, Mar. 2012, doi: https://doi.org/10.1364/OE.20.007118.
[3] A. Elsherif, M. Smigaj, R. Gaulton, J.-P. Gastellu-Etchegorry, and A. Shenkin, "Deriving vegetation indices for 3D canopy chlorophyll content mapping using radiative transfer modelling," Forests, vol. 15, no. 11, art. no. 1878, Nov. 2024, doi: https://doi.org/10.3390/f15111878.
[4] G. Hu, Y. Zhou, Z. Xiang, L. Zhao, G. Chen, T. Li, J. Zhu, and K. Hu, "Fast and accurate generation method of geometric digital twin model of RC bridge with box chambers based on terrestrial laser scanning," Remote Sens., vol. 15, no. 18, art. no. 4440, Sep. 2023, doi: https://doi.org/10.3390/rs15184440.
[5] E. Kaartinen, K. Dunphy, and A. Sadhu, "LiDAR-based structural health monitoring: Applications in civil infrastructure systems," Sensors, vol. 22, no. 12, art. no. 4610, Jun. 2022, doi: https://doi.org/10.3390/s22124610.
[6] D. Merkle and A. Reiterer, "Automated method for SLAM evaluation in GNSS-denied areas," Remote Sens., vol. 15, no. 21, art. no. 5141, Oct. 2023, doi: https://doi.org/10.3390/rs15215141.
[7] A. Wehr and U. Lohr, "Airborne laser scanning—an introduction and overview," ISPRS J. Photogramm. Remote Sens., vol. 54, no. 2–3, pp. 68–82, Jul. 1999, doi: https://doi.org/10.1016/S0924-2716(99)00011-8.
[8] Y. Reshetyuk, Self-calibration and direct georeferencing in terrestrial laser scanning. Stockholm, Sweden: KTH Royal Institute of Technology, 2005.
[9] A. Abellán, J. M. Vilaplana, and J. Martínez, "Application of a long-range terrestrial laser scanner to a detailed rockfall study at Vall de Núria (Eastern Pyrenees, Spain)," Eng. Geol., vol. 88, no. 3–4, pp. 136–148, Dec. 2006, doi: https://doi.org/10.1016/j.enggeo.2006.09.012.
[10] L. Weidner, G. Walton, and C. Phillips, "Investigating the influences of precipitation, snowmelt, and freeze-thaw on rockfall in Glenwood Canyon, Colorado using terrestrial laser scanning," Landslides, vol. 21, no. 9, pp. 2073–2091, Sep. 2024, doi: https://doi.org/10.1007/s10346-024-02266-0.
[11] J. Liu, D. Willkens, and R. Gentry, "Developing a practice-based guide to terrestrial laser scanning (TLS) for heritage documentation," Heritage, vol. 8, no. 8, art. no. 313, Aug. 2025, doi: https://doi.org/10.3390/heritage8080313.
[12] W. R. M. Flynn, H. J. F. Owen, S. W. D. Grieve, and E. R. Lines, "Quantifying vegetation indices using terrestrial laser scanning: Methodological complexities and ecological insights from a Mediterranean forest," Biogeosciences, vol. 20, no. 13, pp. 2769–2784, Jul. 2023, doi: https://doi.org/10.5194/bg-20-2769-2023.
[13] W. Zhang, Z. Chen, R. Huang, Z. Dong, L. Jiang, Y. Xia, B. Chen, and H. Wang, "Multiobjective optimization-based terrestrial laser scanning layout planning for landslide monitoring," IEEE Trans. Geosci. Remote Sens., vol. 61, pp. 1–15, 2023, doi: https://doi.org/10.1109/TGRS.2023.3278471.

[14] L. Cui, X. Luo, Q. Wang, G. Lv, J. Liu, X. Zhang, and Q. Xie, "Enhanced tunnel construction safety: Drill-and-blast construction tunnel deformation detection using LiDAR and cloth simulation filter," Meas. Sci. Technol., vol. 36, no. 9, art. no. 096012, Sep. 2025, doi: https://doi.org/10.1088/1361-6501/ae080b.
[15] M. Fotheringham and D. R. Paudyal, "Combining terrestrial scanned datasets with UAV point clouds for mining operations," ISPRS Ann. Photogramm. Remote Sens. Spatial Inf. Sci., vol. V-4-2021, pp. 129–138, Jun. 2021, doi: https://doi.org/10.5194/isprs-annals-V-4-2021-129-2021.
[16] L. Courtial-Manent, L. Ravanel, J.-L. Mugnier, P. Deline, A. Lhosmot, A. Rabatel, P.-A. Duvillard, and P. Batoux, "18-years of high-Alpine rock wall monitoring using terrestrial laser scanning at the Tour Ronde east face, Mont-Blanc massif," Environ. Res. Lett., vol. 19, no. 3, art. no. 034037, Mar. 2024, doi: https://doi.org/10.1088/1748-9326/ad281d.
[17] A. Algadhi, P. Psimoulis, A. Grizi, and L. Neves, "Experimental assessment of the performance of terrestrial laser scanners in monitoring the geometric deformations in retaining walls," J. Civ. Struct. Health Monit., vol. 15, no. 6, pp. 1885–1900, 2025, doi: https://doi.org/10.1007/s13349-025-00916-y.
[18] R. F. Salcedo Cerquin, M. Alarcon, and R. M. Delgadillo, "BrIM and digital twin integration for structural health monitoring and analysis of the Villena Rey Bridge via laser scanning," Appl. Sci., vol. 15, no. 21, art. no. 11741, 2025, doi: https://doi.org/10.3390/app152111741.
[19] J. Zhu, D. Wang, Z. Fu, Z. Zhang, and W. Han, "BIM-based terrestrial laser scanning path planning for large-scale civil infrastructure," Autom. Constr., vol. 178, art. no. 106439, 2025, doi: https://doi.org/10.1016/j.autcon.2025.106439.
[20] M. Camara, L. Wang, and Z. You, "Three-dimensional point cloud displacement analysis for tunnel deformation detection using mobile laser scanning," Appl. Sci., vol. 15, no. 2, art. no. 625, 2025, doi: https://doi.org/10.3390/app15020625.
[21] N. Tárrago Garay, J. C. Jimenez Fernandez, R. San Mateos Carreton, M. A. Montes Grova, O. Kruth, and P. Elguezabal, "Integration of drone-based 3D scanning and BIM for automated construction progress control," Buildings, vol. 15, no. 19, art. no. 3487, 2025, doi: https://doi.org/10.3390/buildings15193487.
[22] S. W. Nazari, "Yersel lazer tarayıcılar: Geomatik mühendisliğinde uygulama örneği" [Terrestrial laser scanners: An application example in geomatics engineering], M.S. thesis, Dept. Geomatics Eng., Zonguldak Bülent Ecevit Univ., Zonguldak, Turkey, 2020.